Polysaccharide of *Atractylodes macrocephala* Koidz alleviate lipopolysaccharide-stimulated liver inflammation injury of goslings through miR-223/NLRP3 axis

Feiyue Chen,[*,†] Bingxin Li,[*,†] Wanyan Li,[*,†] Wenbin Chen,[*,†] Yunmao Huang,[*,†] Yunbo Tian,[*,†] Baohe Yang,[‡] Mingfeng Yuan,[‡] Danning Xu,[*,†] and Nan Cao[*,†,1]

[*]*College of Animal Science & Technology, Zhongkai University of Agriculture and Engineering, Guangzhou 510225, China;* [†]*Guangdong Province Key Laboratory of Waterfowl Healthy Breeding, Guangzhou 510225, China; and* [‡]*Yunnan Kuaidaduo Animal Husbandry Technology Co., Ltd, Yuxi 653100, China*

ABSTRACT Lipopolysaccharide (**LPS**) infection could cause severe liver inflammation and lead to liver damage, even death. Previous studies have shown that polysaccharide of *Atractylodes macrocephala* Koidz (**PAMK**) could protect liver from inflammation caused by LPS in mice. However, whether PAMK could alleviate liver inflammatory injury in other animals with LPS is still unknown. For evaluating whether PAMK could alleviate liver inflammatory injury in goslings with LPS, a total of 80 healthy 1-day old Magang goslings were randomly divided into 4 groups (control group, PAMK group, LPS group, and PAMK+LPS group). Goslings in control group and LPS group were fed with basal diet, and goslings in PAMK group and PAMK+LPS group were fed basal diet supplemented with 400 mg/kg PAMK to the end of trial. On 24 d of age, goslings in the control group and PAMK group were intraperitoneal injected 0.5 mL normal saline, and goslings in LPS and PAMK+LPS groups were intraperitoneal injected with LPS at 5 mg/kg BW. The serum and liver samples were collected for further analysis after treatment of LPS at 6, 12, 24, and 48 h. Furthermore, the hepatocytes were extracted from goose embryo to measure the expression of the key genes of miR-223/NLRP3 axis. The results showed that PAMK pretreatment could maintain normal cell morphology of liver, alleviate the enhanced levels of biochemical indexes ALT and AST, decrease the levels of IL-1β and IL-18, increase the relative mRNA expression of miR-223, and decrease the expression of NLRP3, Caspase-1, and cleaved Caspase-1 in liver and hepatocytes of goslings induced by LPS. These results indicated that PAMK could relieve inflammatory liver tissue damage after LPS treatment and downregulate the level of inflammation factors via miR-223/NLRP3 axis, thus playing a liver protective role in liver inflammation injury in goslings.

Key words: polysaccharide of *Atractylodes macrocephala* Koidz, miR-223/NLRP3 axis, lipopolysaccharide, gosling, liver inflammation

2023 Poultry Science 102:102285
https://doi.org/10.1016/j.psj.2022.102285

INTRODUCTION

During the cultivation of goslings, feed corruption and poor breeding environment could cause widespread bacterial infection. This phenomenon will increase blood levels of endotoxin lipopolysaccharide (**LPS**) in goslings, and LPS exposure could greatly impact both product quality and consumer palatability (Herrera et al., 2021). More importantly, LPS could stimulate the innate immunity and trigger biochemical and cellular responses that lead to the inflammation and toxicity (Kolomaznik et al., 2017). The immature immune system makes goslings vulnerable to LPS, which may lead to serious liver damage or death and reduce production performance and economic benefits. Liver is an important organ for the body to build an organic connection between the innate and adaptive immunity. And it is the main organ for metabolism and excretion (Sarkar et al., 2012). Within the liver, all resident cells are able to respond to LPS (Schippers et al., 2020). Exposure to high levels of LPS in the liver can lead to the recruitment of inflammatory cells, destroying the parenchyma of the liver (Farghali et al., 2015). Therefore, maintaining homeostasis and keeping the function of liver properly is crucial to preventing disease occurrence and improving the quality of cultured goslings.

Received August 3, 2022.
Accepted October 19, 2022.

[1]Corresponding author: caonan870405@126.com

Chinese medicine polysaccharide is the extract of Chinese herbal medicine, which is gradually being paid close attention due to its beneficial features including multitarget effects, rich resources, less side effects and safety (Schepetkin and Quinn, 2006). Polysaccharide of *Atractylodes macrocephala* Koidz (**PAMK**) is the main active ingredient of *Atractylodes macrocephala* which has been shown to have the ability to regulate the immune functions (Xu et al., 2017; Hou et al., 2020). More importantly, PAMK could protect liver injury caused by various reasons. Some research showed that PAMK could reduce the elevated expression of markers of liver dysfunction and the hepatic morphologic changes induced by hepatic ischemia-reperfusion injury in rats (Jin et al., 2011). Other studies have found that PAMK has a certain protective effect on the CCl4-induced liver injury in mice; the protective effect may be related to its anti-oxidation, its inhibition of NOS activity and NO level, and its reduction in the production of free radicals (Han et al., 2016). The hepatoprotective effect of PAMK has been presented in diverse models of liver injury.

Nucleotide-binding domain-like receptor protein 3 (**NLRP3**) inflammasome activation is involved in various liver diseases (Shi et al., 2020a). NLRP3 inflammasome is a cytosolic complex for early inflammatory responses that sense microbes and endogenous danger signals (Stutz et al., 2017). LPS stimulation induces activation of the NLRP3 inflammasome (Boaru et al., 2012). The activation of the NLRP3 inflammasome triggers Caspase-1 activation, subsequently, leads to the processing of IL-1β and IL-18, which contributes to an exacerbated inflammatory response (Basic et al., 2017; Clark et al., 2018). miR-223 is a negative regulator of inflammation and a highly conserved miRNA among species, which could bind to the 3′-UTR of the NLRP3 mRNA and regulate gene expression by inhibiting NLRP3 mRNA translation to effect the process of inflammation (Bauernfeind et al., 2012; Zhao et al., 2018). Furthermore, it was reported that miR-223 was downregulated in injury models induced by LPS (Li et al., 2019b; Tan et al., 2020). More importantly, many research have certificated that herbal polysaccharides could attenuate inflammatory injury through suppressing the expression of NLRP3 inflammasome (Tian et al., 2017; Zhao et al., 2021). However, no information is available about the effect and mechanism of PAMK on liver inflammatory injury in goslings caused by LPS. In that case, this study was designed to estimate whether PAMK could attenuate liver injury in goslings caused by LPS and explore the mechanism.

MATERIALS AND METHODS

Experiment Grouping and Treatments

All goslings were treated humanely, and the experiments received prior ethical approval in accordance with Zhongkai University of Agriculture and Engineering under the approved protocol number SRM-2021-0902. 80 goslings were purchased from Guangdong Qingyuan Jinyufeng Goose Co., Ltd. (Qingyuan, China). The goslings were housed in a specific pathogen-free environment and enrolled in experiments at 1 d of age, with half of them male and half female. PAMK without endotoxin (purity 95%) used in this experiment was purchased from Yangling Ciyuan Biotech Co., Ltd. (Xi'an, China). It was freshly prepared every day and then diluted with water and sprayed on the feed according to the concentration of 400 mg/kg. Goslings were randomly divided into 4 groups (control group, PAMK group, LPS group, and PAMK+LPS group) with 4 replicates per group and 5 goslings per replicate in a single-factor completely randomized experimental design. The goslings had free access to food (including vegetables) and water. The control and LPS groups were fed normal diets. Whereas goslings in PAMK and PAMK+LPS groups were fed the normal diet supplemented with 400 mg/kg PAMK from 1 d of age to the end of the trial. On 24 d of age, goslings in the control and PAMK groups were intraperitoneal injected 0.5 mL normal saline, and goslings in LPS and PAMK+LPS groups were intraperitoneal injected with LPS (Escherichia coli 055: B5; Sigma, St. Louis, MO) at 5 mg/kg BW, respectively. After treatment of LPS at 6, 12, 24, and 48 h, blood was drawn from randomly 5 goslings in each group to isolate serum. Then the goslings were euthanized, and part of the same leaf liver tissue of each gosling was fixed in 4% paraformaldehyde. The remaining part of liver was collected and frozen in liquid nitrogen and stored at -80°C until further analysis.

Histologic Analysis

The tissues were embedded in paraffin. Paraffin-fixed blocks were serially sectioned into 5 μm-thick slices. Sections were stained with hematoxylin and eosin (**H.E.**) for histological examination and visualized under a Nikon ECLIPSE E100 microscope (Tokyo, Japan).

Serum Biochemical Indexes Analysis

The alanine aminotransferase (**ALT**) and aspartate aminotransferase (**AST**) were measured by a VetScan VS2 chemistry analyzer (ABAXIS, Union City, CA) and used as indicators for liver damage.

Culture and Treatments of Hepatocytes

Primary goose embryo hepatocytes were isolated and cultured after collagenase type Ⅳ (2091GR001, BioFROXX, Einhausen, Germany) digestion of the liver. Hepatocytes were adjusted to a density of 10^6 cells/mL and cultured in a 6-well plate (Corning Incorporated, Steuben County, NY) with DMEM (SH30022.02, Hyclone, Logan, UT) containing 10% FBS (10100147, Gibco, AUS). Hepatocytes were incubated for 24 h at 39°C with 5% CO_2. Subsequently, all groups were replaced the culture medium. Of these, the cells in the

PAMK and PAMK+LPS groups were pretreated with 40 μg/mL PAMK for 12 h. After the medium was changed, 200 μg/mL LPS was added to the LPS and PAMK+LPS groups on the basis of retaining the original PAMK treatment. After exposure to LPS for 24 h, culture medium was collected for analysis the concentrations of cytokines, and cells were harvested for RNA and protein extraction.

Double Luciferase Reporter Gene to Validation of Target Gene

New vectors were constructed based on psiCHECK-2 plasmids. Inserting the target response elements (NLRP3 3'UTR) into psiCHECK-2 and using XhoI/NotI to double digestion. The target fragment was ligated with the vector with T4 ligase, transformed, and the plasmid was digested to identify positive clones and sequenced. Mutating the target locus to a new vector, which was named psiCHECK-2-NLRP3-plasmids. Mutate the binding site of miR-223, repeating the above steps and renaming it mut-psiCHECK-2-NLRP3-plasmids. The 293T cells were co-transfected with the psiCHECK-2-NLRP3-plasmids, mut-psiCHECK-2-NLRP3-plasmids, miR-223-mimic, and corresponding negative mimic (NC mimic) using Lipofectamine 3,000 (L3000015, Invitrogen, Carlsbad, CA). The mut-psiCHECK-2-NLRP3-plasmids sequences were shown in Table 1, the underlined sequence represents the mutation sequence.

Cell Transfection

The miR-223 mimic, corresponding negative mimic (NC mimic), miR-223 inhibitor, and NC inhibitor (Ribobio, Guangzhou, China) were used for the overexpression and inhibition of miR-223 in cells respectively. Hepatocytes were transfected with 20 nM mimic or 100 nM inhibitor in 6-well plates according to the manufacturer's instructions. After transfection for 24 h, cells were harvested for further experiments and the transfected efficiency were evaluated using quantitative real-time quantitative polymerase chain reaction (**PCR**) and western blot.

Rescued experiments were performed to further explore and verify whether miR-223 can target and regulate NLRP3 and the specific role of miR-223/NLRP3 in the process of PAMK alleviating inflammatory liver damage induced by LPS in goslings. Based on the establishment of miR-223 overexpression/inhibition model of hepatocytes, detected the expression levels of NLRP3, Caspase-1 and cleaved Caspase-1 in LPS induced hepatocytes after overexpression of miR-223. On the other hand, cells were treated with the above indicated dose and time of miR-223 inhibitor and used PAMK in an attempt to rescue the inhibitory effects, prior to stimulation with LPS for 24 h.

Concentrations of Inflammatory Cytokine and Analysis

The livers were weighed and 0.86% normal saline was added at a ratio of *1:9* (m:V). The sample was fully broken in sample disrupter (JXFSTPRP-24, Jingxin, Shanghai, China). After centrifugation (3,000 *r/min*, 4°C, 10 *min*), the supernatants were collected for test. Similarly, after centrifugation, the supernatants of culture medium were collected for test. Concentrations of IL-1β (ZK-C6332) and IL-18 (ZK-C6333) in liver and hepatocytes were respectively measured by means of enzyme-linked immunosorbent assay (**ELISA**) kits (Ziker Biological Technology Co., Ltd, Shenzhen, China).

Real-Time Quantitative PCR

Total RNA was extracted by Trizol RNA isolation reagent (15596026, Ambion, Austin, TX). An Epoch 3 microplate spectrophotometer (Bio-Tek, Winooski, VT) was used to detect RNA concentration, and agarose gel electrophoresis was used to measure RNA quality. The mRNA was reverse-transcribed into cDNA according to the instructions of the PrimeScript RT Master Mix (RR036A, Takara, Dalian, China). And the stem-loop method was used for miR-223 reverse transcription according to instructions of ImPro-Ⅱ Reverse Transcription System (A3800, Promega, WI). After that, quantitative real-time polymerase chain reaction assays were conducted on an ABI StepOnePlus Real-Time PCR detection system using a PowerUp SYBR Green Master Mix (Applied Biosystems, Foster City, CA). PCR procedure steps included 95°C for 10 min, followed by 35

Table 1. The sequence of mut-psiCHECK-NLRP3-plasmids.

NLRP3 reference sequence (Gene bank accession number)	Mutation sequence and site
XM_013198346	ctcgagAGAGTAAGGCCGGCAGCAGCCCCCAGGACTCTCCCCAGCTCCGCAAGA GACCGCCCCGATGGCAGCACTAGGCAGGCACCCTGCAGAAGCACCAGTAT GACTGCAAGGAACAATGGGGAGGCTCTCAGTCCTCGACCTAGGCTGCCA CAAAATAAAGATATCTAAAACAAGATGCGTGCCTTTCTTTCCTGGACG GCGTTTCGACTTCCTCCCCTTGTAG**CACTGT**TGACCCCATAAGCCC CAGCTGCCACTTCTGCTCCCTCCAGAGCTATGGCACGGTGGCTGGAG CATCCTTGCTGCTGCTTGTGGCCCCACCAACACCACCCCAG CAGCCCTTCCCTTGGGGTCAGCTGGTGGCAGC TTTGGCTGTCTGTTTGGgcggccgc

Table 2. Primer sequences of target genes.

Gene	Primer sequences (5' → 3')	Product Size, bp
NLRP3	F: GCACTGGAAGGTCTCACACTCG R:CCCTCTGGTTCATCTCCTCAAA	208
β-actin	F: GCACCCAGCACGATGAAAAT R: GACAATGGAGGGTCCGGATT	150
miR-223	RT: CTCAACTGGTGTCGTG-GAGTCGGCAATTCAGTT-GAGGGGGTATTT F: ACACTCCAGCTGGGTGT-CAGTTTGTCAAATA R: CTCAACTGGTGTCGTGGA	195
U6	RT: AACGCTTCACGAATTTGCGT F: CTCGCTTCGGCAGCACA R: AACGCTTCACGAATTTGCGT	84

cycles of 95°C for 15 s, and 55°C for 60 s. The primer sequences for NLRP3, β-actin, miR-223 and U6 were presented in Table 2. All primers were synthesized by BGI (Shenzhen, China). The mRNA expressions of NLRP3 and miR-223 were calculated using the $2^{-\Delta\Delta Ct}$ method after normalization with the reference gene β-actin and U6.

Western Blot Analysis

Antibodies against NLRP3 (1:1,500; WL02635), Caspase-1 (1:1,000; WL03450), cleaved-Caspase-1 (1:1,000; WL02996a) were purchased from Wanleibio Co., Ltd. (Shenyang, China) and antibodies against GAPDH (1:10,000, Ab181602) from Abcam plc. (Cambridge, UK). Total protein from liver tissue was extracted by using Radio Immunoprecipitation Assay buffer and PMSF (Beyotime, Shanghai, China). Protein concentration was determined by the BCA method using the Pierce BCA protein assay kit (23227, Thermo Scientific). The proteins were denatured with SDS-PAGE sample loading buffer (Beyotime, Shanghai, China) at boiling water for 10 min and then cool down at the bench before protein electrophoresis. Samples containing 10 mg proteins were separated by electrophoresis on 12.5% SDS-polyacrylamide gels (PG113, EpiZyme, Shanghai, China). Next, proteins were transferred onto PVDF membranes (88518, Thermo Scientific, Waltham, MA). After blocking with PBST containing 5% skim milk (1172GR500, BioFroxx, Germany), the membrane was then incubated with primary antibody overnight at 4°C and with secondary antibody (goat anti-rabbit IgG H&L 1:10,000; Ab6721, Abcam, UK) for 1 h at room temperature. Finally, blots were visualized using the *Tanon 5200* system (*Tanon*, Shanghai, China). Quantitative image analysis was accomplished employing *Image J* 1.52v Software (National Institutes of Health, Bethesda, MA).

Statistical Analysis

All data were assessed by one-way analysis of variance procedure using SPSS statistical software (Ver. 20.0 for windows, SPSS, Chicago, IL). The differences between several groups were analyzed by one-way ANOVA followed by the Tukey multiple-comparison test for unequal replications. A level of $P < 0.05$ indicated that the difference was statistically significant. Results were presented as means ± SD.

RESULT

Hepatic Morphology

At the 6 to 48 h after LPS treatment, the hepatic cords were arranged neatly, the structure and morphology of hepatocytes were normal, and the nucleoli was clear in control group and PAMK group (Figures 1A−1H). Compared with the control group, histopathologic analysis in LPS group of the hepatic tissue revealed hyperemia, and dilatation of hepatic sinusoids (Figure 1I). Compared with LPS group, hepatic sinusoids of PAMK+LPS group became narrow, and portal area exhibited good morphology (Figure 1M). At 12 h after LPS injection, the number of fat vacuoles in the hepatocyte increased, and the structures of the hepatic cords were not clear in LPS group (Figure 1J). But the hepatic cords of PAMK+LPS group was neat and orderly (Figure 1N). At 24 h after LPS injection, LPS induced severe steatosis with severe fat vacuoles in the hepatic tissue (Figure 1K). However, in PAMK+LPS group, the liver steatosis significantly attenuated, and the structure of hepatic cords and hepatic sinusoids returned to normal (Figure 1O). At 48 h after LPS injection, a large amount of inflammatory cell infiltration in liver tissues, the hepatic cords arranged in disorder, the cytoplasm became less, and the hepatocyte morphological structure was unclear in the LPS group (Figure 1L). But the pathological changes in the liver histology had obviously improved in PAMK+LPS group (Figure 1P).

Activities of ALT and AST in Serum

ALT and AST in serum were determined to examine LPS-induced liver function. As shown in Figure 2, the level of serum ALT was significantly higher in the LPS-treated goslings compared with the control group at 12 to 48 h after LPS injection ($P < 0.05$). However, the level of ALT in the serum of the PAMK+LPS group significant decreased compared with the LPS group ($P < 0.05$). Likewise, LPS-induced liver injury increased serum AST levels, which decreased by PAMK pretreatment in the PAMK+LPS group.

Concentration of Cytokines in Liver

As shown in Figure 3, during 24 to 48 h after LPS treatment, the IL-1β level of LPS group increased. Likewise, LPS also increased level of IL-18 in liver tissue. In addition, compared with control group, the levels of IL-1β and IL-18 in LPS group were reached a maximum level at 24 h after LPS injection ($P < 0.05$). Compare

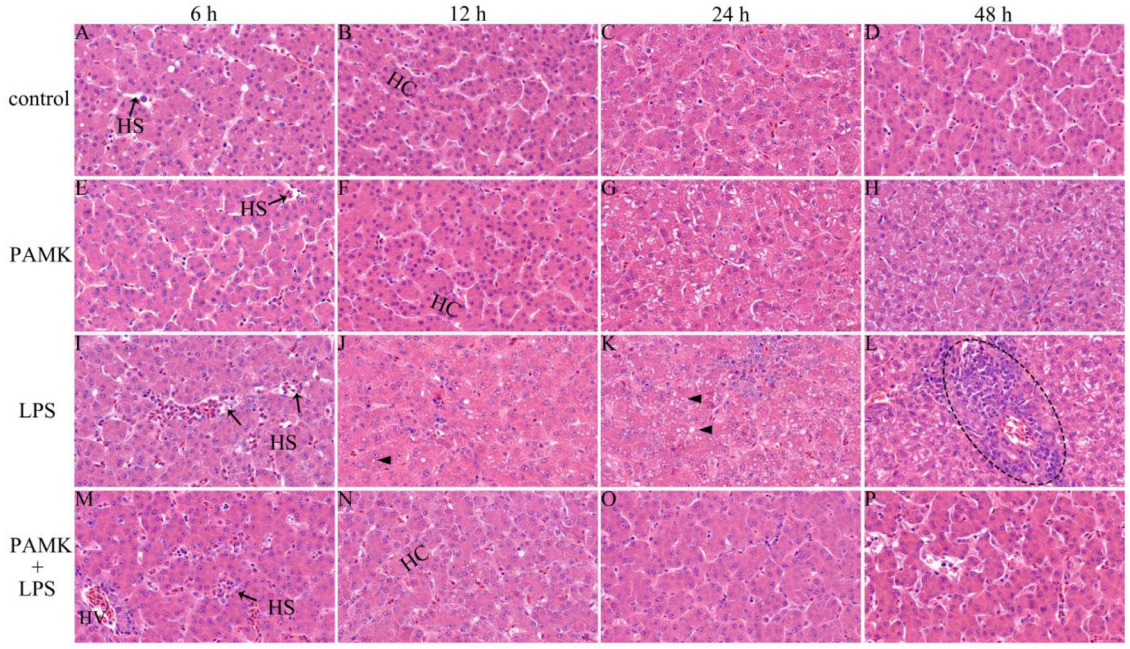

Figure 1. Result of H.E. staining of goslings liver (H.E. staining, 660 ×). (A−D) control group; (E−H) PAMK group; (I−L) LPS group; (M−P) PAMK + LPS group; the images from left to right show the liver at 6 h, 12 h, 24 h, and 48 h after LPS treatment. Control, LPS group fed a basal diet; PAMK, PAMK+LPS group fed a diet supplemented with PAMK at 400 mg/kg. Abbreviations: HS, hepatic sinusoid; HC, hepatic cords; HV, hepatic venule; triangle, *fat vacuole;* circle, inflammatory cell infiltration.

with LPS group, PAMK pretreatment decreased the LPS-induced production of IL-1β and IL-18 in the PAMK+LPS group.

Hepatic mRNA Expressions of miR-223 and NLRP3

As shown in Figure 4, compared with control group, relative expression of miR-223 in LPS group significantly decreased at 24 h after LPS treatment ($P < 0.05$). But the expression of miR-223 in PAMK+LPS group was recovered to normal level after PAMK pretreatment ($P < 0.05$). Besides, the expression of NLRP3 in the LPS group increased after LPS treatment and extremely significant increased at 12 and 24 h ($P < 0.05$). Specifically, the mRNA relative expression of NLRP3 in PAMK +LPS group significantly decreased at 6 to 24 h ($P <$ 0.05).

Hepatic Protein Expressions of NLRP3 and Downstream Genes

As presented in Figure 5, compared with control group, the protein expression levels of NLRP3, Caspase-1 and cleaved Caspase-1 in LPS group slightly increased at 6 h and 12 h, and significant increased at 24 and 48 h after LPS treatment ($P < 0.05$). Compared with LPS group, the protein expression levels of NLRP3, Caspase-1 and cleaved Caspase-1 in PAMK+LPS group were decreased at 24 and 48 h after LPS treatment. In which, the NLRP3 and Caspase-1 expression were significantly decreased at 48 h after LPS treatment ($P < 0.05$).

Concentration of Cytokines in Hepatocytes

As shown in Figure 6, compare with the control group, the levels of IL-1β and IL-18 in the LPS group were

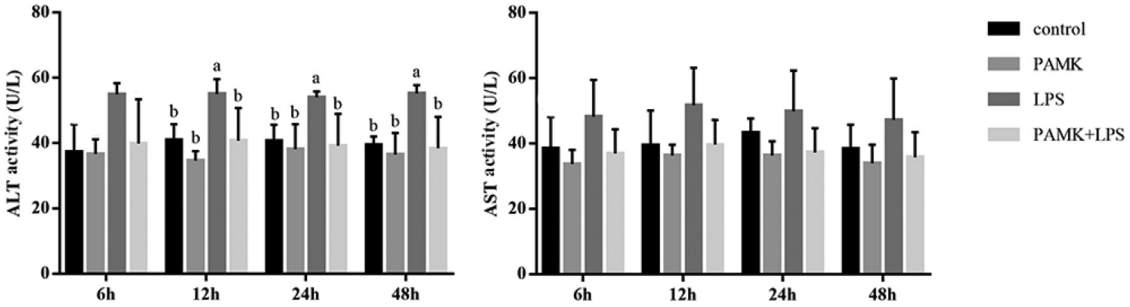

Figure 2. Effect of PAMK on the activities of serum ALT and AST in goslings with liver inflammatory injury. Data are expressed as the means ± SD, n = 5. Different letters mean significant difference ($P < 0.05$); the same letter indicates no significant difference ($P > 0.05$). Abbreviations: ALT, alanine aminotransferase; AST, aspartate aminotransferase.

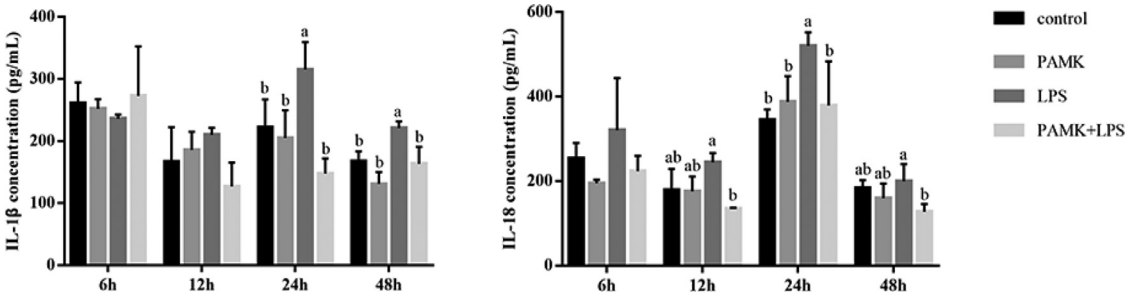

Figure 3. Effect of PAMK on the cytokines concentration of IL-1β and IL-18 in hepatic tissue. Data are expressed as the means ± SD, n = 5. Different letters mean significant difference ($P < 0.05$); the same letter indicates no significant difference ($P > 0.05$).

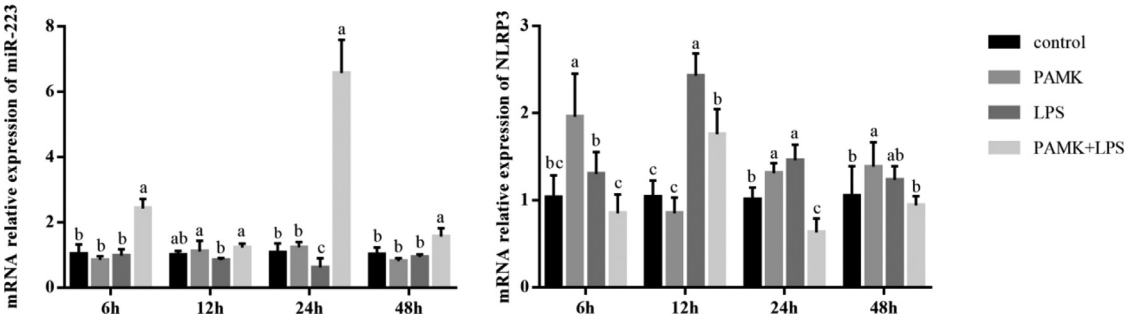

Figure 4. Effects of PAMK on mRNA relative expression of miR-223 and NLRP3 in the hepatic tissue. Data are expressed as the means ± SD, n = 5. Different letters mean significant difference ($P < 0.05$); the same letter indicates no significant difference ($P > 0.05$).

significantly increased after LPS stimulation ($P < 0.05$). Compare with the LPS group, PAMK pretreatment significantly decreased the LPS-induced production of IL-1β and IL-18 in the PAMK+LPS group ($P < 0.05$).

Dual Luciferase Reporter Gene Validation miR-223 Targets NLRP3

The double fluorescence detection results are shown in Figure 7A. When miR-223 was co-transfected with wild-type NLRP3, the R/F value was significantly lower than the NC group and mut-NLRP3 group. It showed that miR-223 interacted with wild-type NLRP3. The results indicated that miR-223 targets NLRP3.

Transfection Efficiency Detected by Real-Time Quantitative PCR and Western Blot

As shown in Figure 7B, the transfection efficiency was achieved 100 times after overexpression of miR-223 in hepatocytes. And Figure 7C shows that the interference efficiency was more than 50%. The results showed that these synthetic sequences could be used for miR-223 overexpression/inhibition experiments in hepatocytes. Besides, as shown in Figures 7D−7F, the mRNA and protein expression of NLRP3 was significantly decreased in miR-223 mimic group ($P < 0.05$). On the other side, Figures 7G−7I shows that the mRNA and protein expression of NLRP3 was significantly increased in miR-223 inhibitor group ($P < 0.05$). The results showed that overexpressed or inhibited the expression of miR-223 could reverse the expression of NLRP3.

miR-223 Could Inhibit LPS-Induced Expression of NLRP3 and Downstream Genes in Hepatocytes

As shown in Figure 8, the expression of NLRP3 was significantly enhanced by LPS stimulation. Transfection of miR-233 mimic inhibited the upregulation of LPS-induced NLRP3, Caspase-1 and cleaved Caspase-1. In addition, we found miR-223 overexpression could effectively inhibit the mRNA and protein expression of NLRP3 induced by LPS ($P < 0.05$).

Inhibiting miR-223 Could Reverse the Effect of PAMK on the Expression of NLRP3 and Downstream Genes in LPS Induced Hepatocytes

As shown in Figure 9, inhibiting the expression of miR-223 could reverse the effect of PAMK on LPS induced gosling embryonic hepatocytes and up regulate the expression levels of NLRP3 and cleaved Caspase-1.

DISCUSSION

Many natural polysaccharides derived from plants possess proven biological properties, including anti-tumor, anti-oxidant, anti-bacterial, and anti-inflammatory

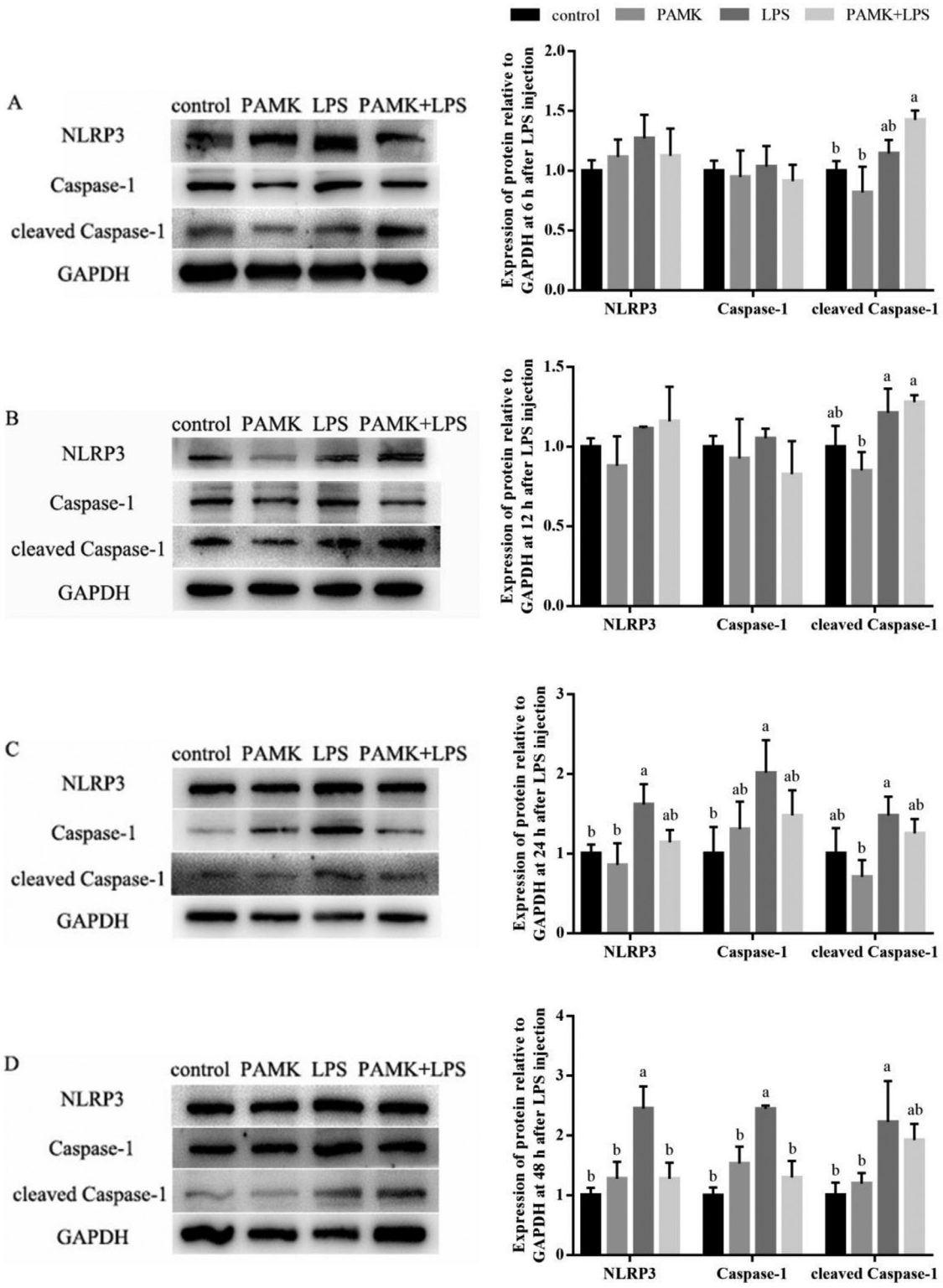

Figure 5. Effect of PAMK on protein relative expression levels of NLRP3, Caspase-1 and cleaved Caspase-1 in the hepatic tissue. (A) Expression of protein relative to GAPDH at 6 h after LPS treatment. (B) Expression of protein relative to GAPDH at 12 h after LPS treatment. (C) Expression of protein relative to GAPDH at 24 h after LPS treatment. (D) Expression of protein relative to GAPDH at 48 h after LPS treatment. Data are expressed as the means ± SD, n = 5. Different letters mean significant difference ($P < 0.05$); the same letter indicates no significant difference ($P > 0.05$).

(Schepetkin and Quinn, 2006; Li et al., 2021a). The chemical investigations on the *Atractylodes macrocephala* Koidz have demonstrated immunoregulatory activities and relieving heat stress (Li et al., 2021a). Studies have found that PAMK might decrease the production of IL-6 and TNF-α, increase the level of superoxide dismutase, and improve the renal tissue injury (Xia et al., 2020). Li found that PAMK could relieve LPS-induced gosling enteritis by maintaining the small intestine morphology and decrease the level of IL-1β, IL-6, TNF-α, and immunoglobulin

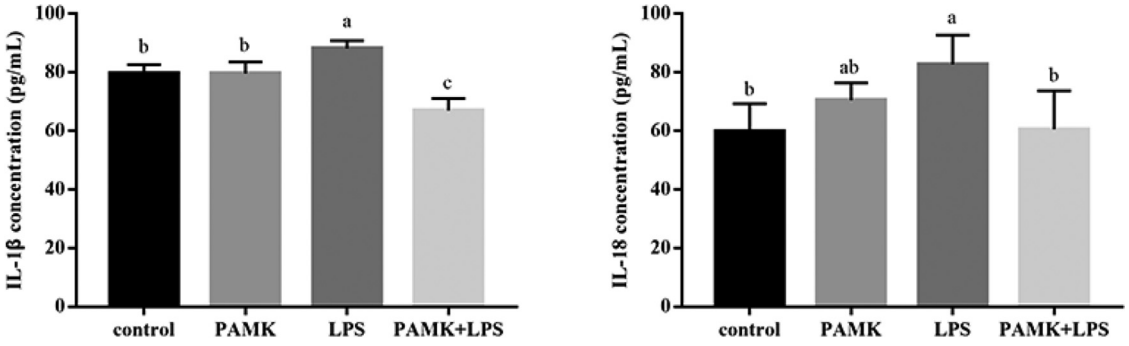

Figure 6. Effect of PAMK on the concentration of IL-1β and IL-18 in hepatocytes by LPS-stimulated. Data are expressed as the means ± SD, n = 6. Different letters mean significant difference ($P < 0.05$); the same letter indicates no significant difference ($P > 0.05$).

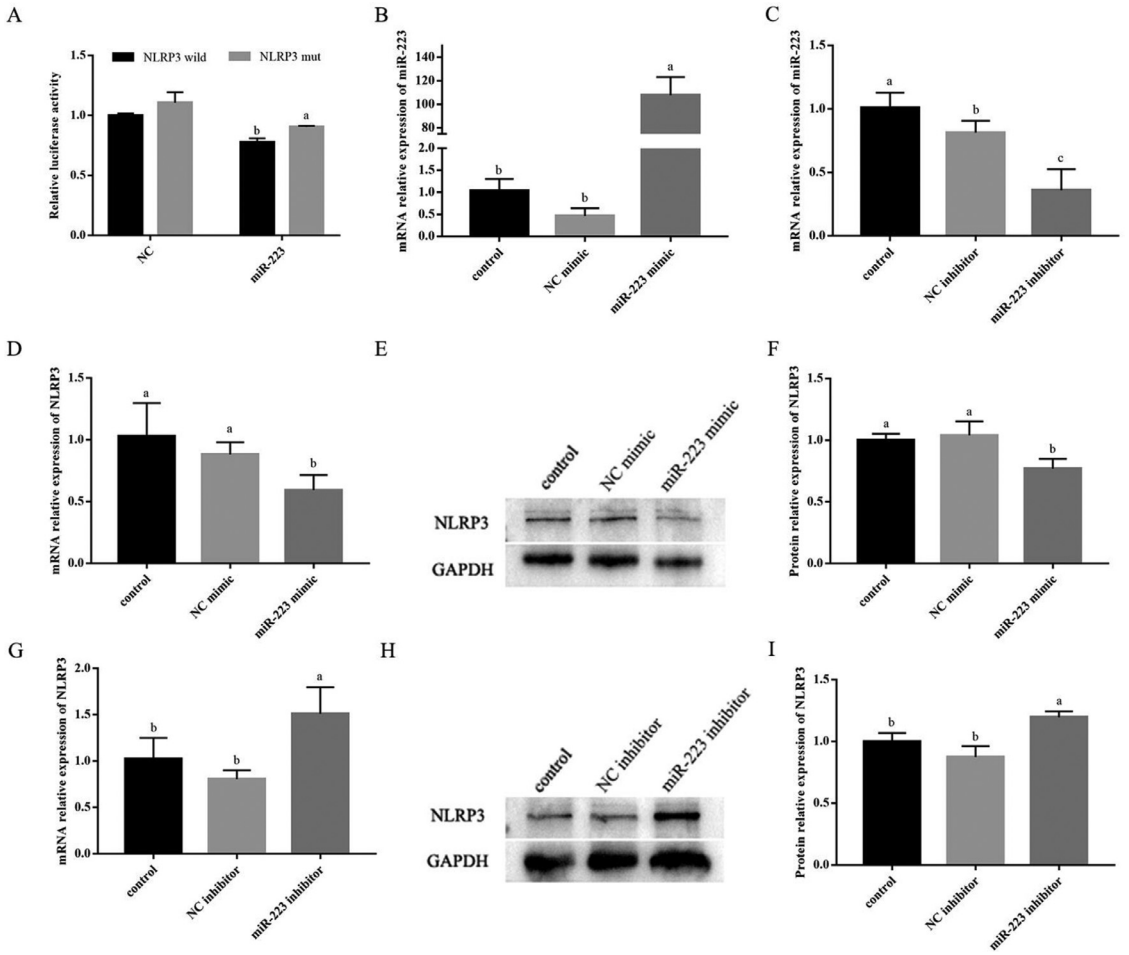

Figure 7. miR-223 could inhibit the expression of NLRP3. (A) Comparison of relative fluorescence values between wild-type and mutant plasmids. (B & D) The efficiency of the miR-223 mimic in hepatocytes was detected by real-time quantitative PCR. (C & G) The efficiency of the miR-223 inhibitor in hepatocytes was detected by real-time quantitative PCR. (E & F) The efficiency of the miR-223 mimic in hepatocytes was detected by western blot. (H & I) The efficiency of the miR-223 inhibitor in hepatocytes was detected by western blot. Data are expressed as the means ± SD, n = 3. Different letters mean significant difference ($P < 0.05$); the same letter indicates no significant difference ($P > 0.05$).

relatively stable and improving the disorder of intestinal flora (Li et al., 2021b). Furthermore, Li's research suggests that PAMK may increase immune-response capacity of the spleen in mice through TLR4-MyD88-NFκB pathway (Li et al., 2019a). This study confirms that PAMK plays a preventive role to protect effects against LPS-induced hepatic injury.

LPS is the main toxic substance produced by Gram-negative bacteria, which severely impair extensive physiological activities in both avians and mammals, including causing sickness behavior, reductions in immune function, embryo mortality and even death (Jiang et al., 2011). LPS-binding protein is produced mainly by the liver and helps mediate the *LPS*-induced inflammatory response (Grube et al., 1994). Liver is the central organ of metabolism (Nguenang et al., 2020). Hepatic morphology reflects the liver health which can be assessed by steatosis, fibrosis, hyperemia or degree of

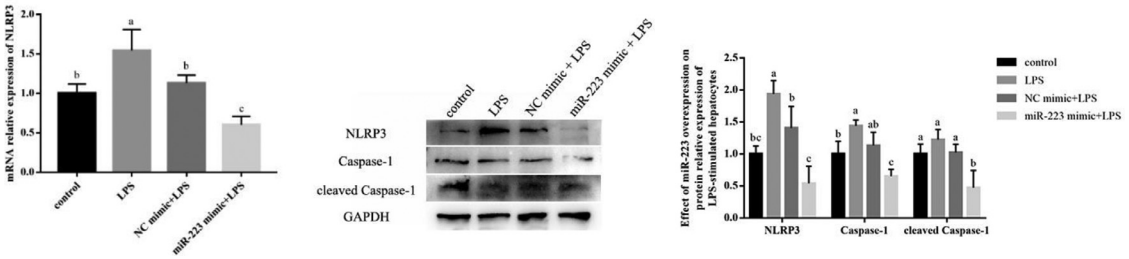

Figure 8. Effect of miR-223 overexpression on the expression of NLRP3 and downstream genes in hepatocytes by LPS-stimulated. Data are expressed as the means ± SD, n = 4. Different letters mean significant difference ($P < 0.05$); the same letter indicates no significant difference ($P > 0.05$).

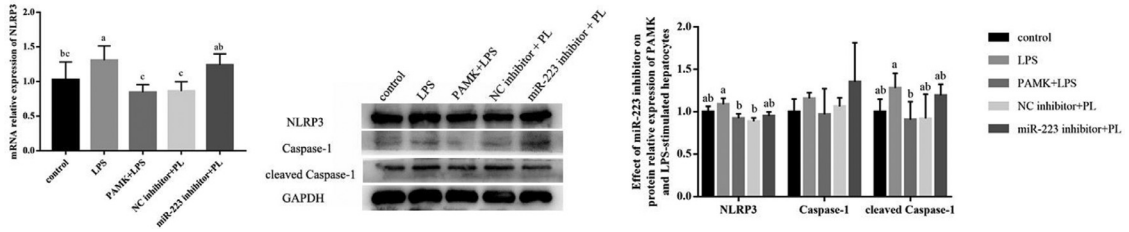

Figure 9. Effect of PAMK treatment on the expression of NLRP3, Caspase-1 and cleaved Caspase-1 in hepatocytes by LPS-stimulated after miR-223 inhibition. PL: PAMK+LPS group. Data are expressed as the means ± SD, n = 4. Different letters mean significant difference ($P < 0.05$); the same letter indicates no significant difference ($P > 0.05$).

inflammatory cell infiltration (*Hermenean et al., 2012*; *Zhang et al., 2018*; *Wang et al., 2021*). In this experiment, LPS mainly caused hyperemia and inflammatory cell infiltration in liver at 6 h and 12 h after LPS injection. Obvious pathological changes were observed at 24 h after LPS injection. It was showed that LPS caused hepatic steatosis and inflammatory focus were occurred. But at 48 h, the effect of LPS on inducing hepatic inflammatory responses was slightly weakened. In contrast, there were fewer histological abnormalities of hepatocytes in the LPS group with unclear hepatic cords and inflammatory cell infiltration, whereas the fat droplets disappeared. These results were similar to what was observed in the previous LPS-induced liver injury study (Guo et al., 2021). The previous study demonstrated that LPS-induced liver injury belongs to a class of liver inflammatory response syndromes (Yan et al., 2018). Liver injury is usually accompanied with inflammatory response. ALT and AST are the most sensitive indicators reflecting hepatocellular inflammatory injury (Yang et al., 2017). ALT is a cytosolic enzyme which is mainly presented in the cell cytoplasm, while AST mainly exists in the mitochondria of the hepatocytes, plasma AST content will significantly increase only when hepatocytes are severely damaged (Tang et al., 2017; Du et al., 2019). Similar results were found in our study: LPS could cause increasing levels of ALT and AST of gosling. Furthermore, we observed that PAMK supplementation reduced serum AST and ALT levels, which played a protective role in liver inflammation damage caused by LPS, consistent with the histopathological results. These data above suggested that PAMK could improve the hepatic morphology and protected goslings against LPS-induced hepatic damage. miR-223 is regarded as a negative regulator of inflammation in many inflammatory diseases, infections and cancers (Wang et al., 2018; Zhou et al., 2018). Zhang's research proved that feeding miR-223 gene-deficient mice with a high-fat diet leads to nonalcoholic fatty liver disease, which exhibits steatosis, inflammation, fibrosis, and liver cancer (Zhang et al., 2018). Further research also found that when high-fat diet was added, the deletion of miR-223 gene also increased the expression of Cxcl10, Taz and other inflammatory genes and cancer-related genes in mouse hepatocytes (He et al., 2019). Wang's findings demonstrated that overexpression of miR-223 significantly attenuated macrophage foam cell formation, lipid accumulation, and pro-inflammatory cytokine production, whereas transfection with an anti-miR-223 inhibitor reversed this phenomenon, finally demonstrated that the upregulation of miR-223 might block TLR4 signaling by activating the PI3K/AKT pathway, thereby ending the development of atherosclerosis (Wang et al., 2015). NLRP3 is an inflammasome, a multi-protein complex assembled from pattern recognition receptors in the cytoplasm and is a key component of the innate immune system's defense against the host. Generally, NLRP3 is a multiprotein complex assembled in response to infection, cellular injury, or environmental stress. It was reported that NLRP3 overexpression results in severe liver inflammation and fibrosis (Chen et al., 2020). Thus, to ease the inflammatory process and reduce tissue damage, the activation of the NLRP3 inflammasome should be tightly controlled (Lamkanfi and Dixit, 2012). Activation of NLRP3 can promote the development of inflammation by generating Caspase-1, promoting the

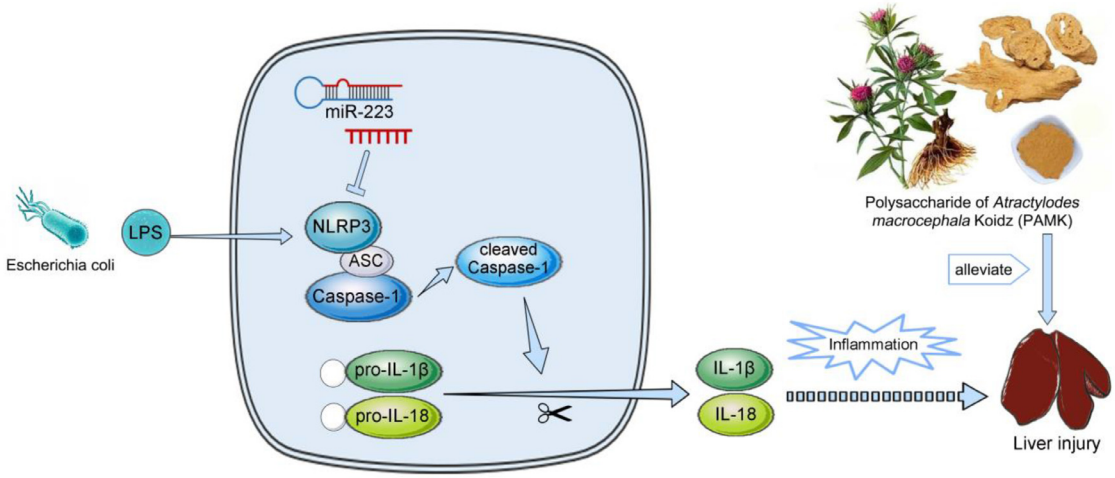

Figure 10. Scheme summarizing the protective effects of PAMK on LPS-induced liver injury via the miR-223/NLRP3 axis.

production of cytokines IL-1β and IL-18 (Shirato et al., 2017).

LPS-stimulated inflammation could activate NLRP3, and miR-223 also plays a role in LPS-induced inflammation and the regulation of inflammasome NLRP3. miR-223 can specifically target the 3′UTR region of NLRP3 mRNA, thereby inhibiting the expression of NLRP3 mRNA (Bauernfeind et al., 2012). Zhao found that the activation of the inflammatory mediator NLRP3 and its mediating effect on IL-1β production could be inhibited by promoting the transcription of miR-223, thereby preventing inflammatory damage (Zhao et al., 2018). It has been reported that miR-223 attenuated LPS-induced lung inflammation in mice via the TLR4/NF-κB and NLRP3 inflammasome signaling pathway (Yan et al., 2019). And the overexpression of miR-223 down-regulates IL-6 and IL-1β expression in TLR-activated macrophages (Wang et al., 2014). IL-1β is an important inflammatory mediator of the inflammatory process (Logan et al., 2007). IL-1β activates additional inflammatory cells and facilitates the release of more inflammatory mediators, which trigger inflammatory cascades and amplify injury signals (Ning et al., 2016). Besides, IL-18 is a pro-inflammatory cytokine that mediates the inflammatory cascade reaction and is a factor in acute liver injury (Tangkijvanich et al., 2007).

In this study, LPS could inhibit the expression of miR-223 and significantly increase the expression of NLRP3 at the same time. More importantly, we found that PAMK pretreatment could significantly up-regulate the expression of miR-223 and decrease the expression of NLRP3 in the PAMK+LPS group. This finding indicated that PAMK could activate the miR-223/NLRP3 axis to attenuate inflammation caused by LPS. The similar studies found that baicalin, sinomenine, and paeonol exerted protective effects on improving inflammation through miR-223/NLRP3 axis (Dong et al., 2019; Sun et al., 2019; Shi et al., 2020b). These *Chinese medicine* extracts could increase the expression of miR-223, thereby directly inhibit NLRP3 expression, and reduce the protein expression of ASC and Caspase-1 and the cytokine expression of IL-1β and IL-18 to alleviate inflammation. The result also showed that PAMK pretreatment could reduce the protein expression of NLRP3 and Caspase-1 and the levels of pro-inflammatory cytokines IL-1β and IL-18 in liver, especially significantly decreased after 24 and 48 h of LPS treatments. This indicates that PAMK pretreatment could activate the miR-223/NLRP3 axis to inhibit inflammation in the later stage. PAMK treatment may better prevent, and attenuate hepatitis caused by LPS.

CONCLUSIONS

In conclusion, the study found that PAMK pretreatment could reduce inflammatory cell infiltration and ameliorated the structure of hepatic cords and hepatic sinusoids, inhibit the levels of ALT and AST in serum induced by LPS, decrease the level of IL-1β and IL-18 in liver. More importantly, PAMK could improve the hepatic morphology via miR-223/NLRP3 axis by increasing the relative mRNA expression of miR-223 and decreasing the expression of NLRP3, Caspase-1 and cleaved Caspase-1, which suggested that PAMK might alleviate inflammatory damage of the liver of gosling caused by LPS via miR-223/NLRP3 axis (Figure 10).

ACKNOWLEDGMENTS

This work was supported by Natural Science Foundation of Guangdong Province (General Program, No. 20220501605), Natural Science Foundation of Hunan Province (General Program, No. 2021JJ30312), Science & Technology Planning Project of Guangzhou (No. 201904010076). We thank the support of Guangdong Province Key Laboratory of Waterfowl Healthy Breeding, Guangzhou 510225, China.

DISCLOSURES

The authors declare no conflicts of interest.

REFERENCES

Basic, A., S. Alizadehgharib, G. Dahlén, and U. Dahlgren. 2017. Hydrogen sulfide exposure induces NLRP3 inflammasome-dependent IL-1β and IL-18 secretion in human mononuclear leukocytes in vitro. Clin. Exp. Dent. Res. 3:115–120.

Bauernfeind, F., A. Rieger, F. Schildberg, P. Knolle, J. Schmid-Burgk, and V. Hornung. 2012. NLRP3 inflammasome activity is negatively controlled by miR-223. J. Immunol. 189:4175–4181.

Boaru, S., E. Borkham-Kamphorst, L. Tihaa, U. Haas, and R. Weiskirchen. 2012. Expression analysis of inflammasomes in experimental models of inflammatory and fibrotic liver disease. J. Inflamm. (Lond.) 9:49.

Chen, Y., R. Que, L. Lin, Y. Shen, and Y. Li. 2020. Inhibition of oxidative stress and NLRP3 inflammasome by Saikosaponin-d alleviates acute liver injury in carbon tetrachloride-induced hepatitis in mice. Int. J. Immunopath. Ph. 34:205873842095059.

Clark, S., R. Schmidt, D. Mcdermott, and L. Lenz. 2018. A Batf3/Nlrp3/IL-18 axis promotes natural killer cell IL-10 production during listeria monocytogenes infection. Cell Rep 23:2582–2594.

Dong, H., P. Li, C. Chen, X. Xu, and H. Zhang. 2019. Sinomenine attenuates cartilage degeneration by regulating miR-223-3p/NLRP3 inflammasome signaling. Inflammation 42:1265–1275.

Du, H., S. Zhang, M. He, K. Ming, J. Wang, W. Yuan, and J. Liu. 2019. Evaluation of the therapeutic effect of a flavonoid prescription against rabbit hemorrhagic disease in vivo. Biomed Res. Int. 2019:1–10.

Farghali, H., K. Kgalalelo, L. Wojnarová, and C. Kutinová. 2015. In vitro and in vivo experimental hepatotoxic models in liver research: applications to the assessment of potential hepatoprotective drugs. Physiol. Res. 65:S417–S425.

Grube, B., C. Cochane, R. Ye, C. Green, M. Mcphail, R. Ulevitch, and P. Tobias. 1994. Lipopolysaccharide binding protein expression in primary human hepatocytes and HepG2 hepatoma cells. J. Biol. Chem. 269:8477–8482.

Guo, S., W. Li, F. Chen, S. Yang, Y. Huang, Y. Tian, D. Xu, and N. Cao. 2021. Polysaccharide of Atractylodes macrocephala Koidz regulates LPS-mediated mouse hepatitis through the TLR4-MyD88-NFκB signaling pathway. Int. Immunopharmacol. 98:107692.

Han, B., Y. Gao, Y. Wang, L. Wang, Z. Shang, S. Wang, and J. Pei. 2016. Protective effect of a polysaccharide from Rhizoma Atractylodis Macrocephalae on acute liver injury in mice. Int. J. Biol. Macromol. 87:85–91.

He, Y., S. Hwang, Y. Cai, S. Kim, M. Xu, D. Yang, A. Guillot, D. Feng, W. Seo, X. Hou, and B. Gao. 2019. MicroRNA-223 ameliorates nonalcoholic steatohepatitis and cancer by targeting multiple inflammatory and oncogenic genes in hepatocytes. Hepatology 70:1150–1167.

Hermenean, A., C. Popescu, A. Ardelean, M. Stan, N. Hadaruga, C. Mihali, M. Costache, and A. Dinischiotu. 2012. Hepatoprotective effects of Berberis vulgaris L. extract/β cyclodextrin on carbon tetrachloride-induced acute toxicity in mice. Int. J. Mol. Sci. 13:9014–9034.

Herrera, N., N. Bland, F. Ribeiro, M. Henriott, E. Hofferber, J. Meier, J. Petersen, N. Iverson, and C. Calkins. 2021. Oxidative stress and postmortem meat quality in crossbred lambs. J. Anim. Sci. 99: skab156.

Hou, C., L. Chen, L. Yang, and X. Ji. 2020. An insight into anti-inflammatory effects of natural polysaccharides. Int. J. Biol. Macromol. 153:248–255.

Jiang, D., L. Li, C. Wang, F. Chen, A. Sun, and Z. Shi. 2011. Raising on water stocking density reduces geese reproductive performances via water bacteria and lipopolysaccharide contaminations in "Geese-Fish" production system. Agr. Sci. China 9:1459–1466.

Jin, C., P. Zhang, C. Bao, Y. Gu, B. Xu, C. Li, J. Li, P. Bo, and X. Liu. 2011. Protective effects of Atractylodes macrocephala polysaccharide on liver ischemia-reperfusion injury and its possible mechanism in rats. Am. J. Chin. Med. 39:489–502.

Kolomaznik, M., Z. Nova, and A. Calkovska. 2017. Pulmonary surfactant and bacterial lipopolysaccharide: the interaction and its functional consequences. Physiol. Res. 66:S147–S157.

Lamkanfi, M., and V. M. Dixit. 2012. Inflammasomes and their roles in health and disease. Annu. Rev. Cell Dev. Biol. 28:137–161.

Li, B., W. Li, Y. Tian, S. Guo, Y. Huang, D. Xu, and N. Cao. 2019a. Polysaccharide of Atractylodes macrocephala Koidz enhances cytokine secretion by stimulating the TLR4-MyD88-NF-κB signaling pathway in the mouse spleen. J. Med. Food 22:937–943.

Li, W., X. Xiang, N. Cao, W. Chen, Y. Tian, X. Zhang, X. Shen, D. Jiang, D. Xu, and S. Xu. 2021a. Polysaccharide of atractylodes macrocephala koidz activated T lymphocytes to alleviate cyclophosphamide-induced immunosuppression of geese through novel-mir2/CD28/AP-1 signal pathway. Poult. Sci 100:101129.

Li, W., X. Xiang, B. Li, Y. Wang, L. Qian, Y. Tian, Y. Huang, D. Xu, and N. Cao. 2021b. PAMK relieves LPS-induced enteritis and improves intestinal flora disorder in goslings. Evid-Based. Compl. Alt. 2021:1–16.

Li, X., W. Wei, Z. Zhao, and S. Lv. 2019b. Tripterine up-regulates miR-223 to alleviate lipopolysaccharide-induced damage in murine chondrogenic ATDC5 cells. Int. J. Immunopath. Ph. 33:1–11.

Logan, R., A. Stringer, J. Bowen, S. Yeoh, R. Gibson, S. Sonis, and D. Keefe. 2007. The role of pro-inflammatory cytokines in cancer treatment-induced alimentary tract mucositis: pathobiology, animal models and cytotoxic drugs. Cancer Treat. Rev. 33:448–460.

Nguenang, G., A. Ntyam, and V. Kuete. 2020. Acute and subacute toxicity profiles of the methanol extract of Lycopersicon esculentum L. Leaves (Tomato), a botanical with promising in vitro anticancer potential. Evid-based. Compl. Alt.1–10 2020.

Ning, Y., Z. Peng, B. Li, J. Xia, and X. Lu. 2016. Isoflurane attenuates lipopolysaccharide-induced acute lung injury by inhibiting ROS-mediated NLRP3 inflammasome activation. Am. J. Transl. Res. 8:2033–2046.

Sarkar, R., B. Hazra, and N. Mandal. 2012. Hepatoprotective potential of Caesalpinia crista against iron-overload-induced liver toxicity in mice. Evid-based. Compl. Alternat. Med. 2012:896341.

Schepetkin, I., and M. Quinn. 2006. Botanical polysaccharides: macrophage immunomodulation and therapeutic potential. Int. Immunopharmacol. 6:317–333.

Schippers, M., E. Post, I. Eichhorn, J. Langeland, and K. Poelstra. 2020. Phosphate groups in the lipid A moiety determine the effects of LPS on hepatic stellate cells: a role for LPS-dephosphorylating activity in liver fibrosis. Cells 9:2708.

Shi, C., H. Yang, and Z. Zhang. 2020a. Involvement of nucleotide-binding oligomerization domain-like receptor family pyrin domain containing 3 inflammasome in the pathogenesis of liver diseases. Front. Cell Dev. Biol. 8:139.

Shi, X., X. Xie, Y. Sun, H. He, H. Huang, Y. Liu, H. Wu, and M. Dai. 2020b. Paeonol inhibits NLRP3 mediated inflammation in rat endothelial cells by elevating hyperlipidemic rats plasma exosomal miRNA-223. Eur. J. Pharmacol. 885:173473.

Shirato, K., K. Imaizumi, T. Sakurai, J. Ogasawara, H. Ohno, and T. Kizaki. 2017. Regular voluntary exercise potentiates interleukin-1β and interleukin-18 secretion by increasing Caspase-1 expression in murine macrophages. Mediat. Inflamm.1–11 2017.

Stutz, A., C. Kolbe, R. Stahl, G. Horvath, B. Franklin, O. Ray, R. Brinkschulte, M. Geyer, F. Meissner, and E. Latz. 2017. NLRP3 inflammasome assembly is regulated by phosphorylation of the pyrin domain. J. Exp. Med. 214:1725–1736.

Sun, H., X. Jin, J. Xu, and Q. Xiao. 2019. Baicalin alleviates age-related macular degeneration via miR-223/NLRP3-regulated pyroptosis. Pharmacology 105:28–38.

Tan, J., J. Fan, J. He, L. Zhao, and H. Tang. 2020. Knockdown of LncRNA DLX6-AS1 inhibits HK-2 cell pyroptosis via regulating miR-223-3p/NLRP3 pathway in lipopolysaccharide-induced acute kidney injury. J. Bioenerg. Biomembr. 52:367–376.

Tang, X., R. Wei, A. Deng, and T. Lei. 2017. Protective effects of Ethanolic Extracts from Artichoke, an edible herbal medicine, against acute alcohol-induced liver injury in mice. Nutrients 9:1000.

Tangkijvanich, P., D. Thong-Ngam, V. Mahachai, A. Theamboonlers, and P. Yong. 2007. Role of serum interleukin-

18 as a prognostic factor in patients with hepatocellular carcinoma. World J. Gastroenterol. 13:4345–4349.

Tian, Z., Y. Liu, B. Yang, J. Zhang, H. He, H. Ge, Y. Wu, and Z. Shen. 2017. Astagalus polysaccharide attenuates murine colitis through inhibition of the NLRP3 inflammasome. Planta. Med. 83:70–77.

Wang, H., H. Pan, Z. Hu, C. Xu, and J. Zhao. 2018. MicroRNA-223 inhibits lipopolysaccharide-induced inflammatory response by directly targeting Irak1 in the nucleus pulposus cells of intervertebral disc. IUBMB Life 70:479–490.

Wang, J., X. Bai, Q. Song, F. Fan, H. Zhi, G. Cheng, and Y. Zhang. 2015. miR-223 inhibits lipid deposition and inflammation by suppressing toll-like receptor 4 signaling in macrophages. Int. J. Mol. Sci. 16:24965–24982.

Wang, Y., E. Brodin, K. Nishii, H. Frieboes, and P. Macklin. 2021. Impact of tumor-parenchyma biomechanics on liver metastatic progression: a multi-model approach. Sci. Rep. 11:1710.

Wang, Y., Y. Zhang, J. Huang, X. Chen, X. Gu, Y. Wang, L. Zeng, and G. Y. Yang. 2014. Increase of circulating miR-223 and insulin-like growth factor-1 is associated with the pathogenesis of acute ischemic stroke in patients. Bmc Neurol 14:77.

Xia, P., K. Gao, J. Xie, W. Sun, and W. He. 2020. Data mining-based analysis of Chinese medicinal herb formulae in chronic kidney disease treatment. Evid-based. Compl. Alt.1–14 2020.

Xu, D., B. Li, C. Nan, W. Li, Y. Tian, and Y. Huang. 2017. The protective effects of polysaccharide of Atractylodes macrocephala Koidz (PAMK) on the chicken spleen under heat stress via antagonizing apoptosis and restoring the immune function. Oncotarget 8:70394–70405.

Yan, D., L. Pan, Z. Chen, S. Zhang, Y. Wang, C. Xin, L. Lei, Z. Xuan, and Z. Lei. 2018. Emodin attenuates lipopolysaccharide-induced acute liver injury via inhibiting the TLR4 signaling pathway in vitro and in vivo. Front. Pharmacol. 9:962.

Yan, Y., K. Lu, T. Ye, and Z. Zhang. 2019. MicroRNA223 attenuates LPS induced inflammation in an acute lung injury model via the NLRP3 inflammasome and TLR4/NFκB signaling pathway via RHOB. Int. J. Mol. Med. 43:1467–1477.

Yang, Q., G. Ji, R. Pan, Y. Zhao, and P. Yan. 2017. Protective effect of hydrogen-rich water on liver function of colorectal cancer patients treated with mFOLFOX6 chemotherapy. Mol. Clin. Oncol. 7:891–896.

Zhang, M., Y. Yuan, Q. Wang, X. Li, J. Men, and M. Lin. 2018. The Chinese medicine Chai Hu Li Zhong Tang protects against non-alcoholic fatty liver disease by activating AMPKα. Biosci. Rep. 38: BSR20180644.

Zhao, G., K. Jiang, Y. Yang, T. Zhang, and G. Deng. 2018. The potential therapeutic role of miR-223 in bovine endometritis by targeting the NLRP3 inflammasome. Front. Immunol. 9:1916.

Zhao, Y., Q. Wang, S. Yan, J. Zhou, and T. Zheng. 2021. Bletilla striata polysaccharide promotes diabetic wound healing through inhibition of the NLRP3 inflammasome. Front. Pharmacol. 12:659215.

Zhou, W., A. S. Pal, Y. H. Hsu, T. Gurol, X. Zhu, S. E. Wirbisky-Hershberger, J. L. Freeman, A. L. Kasinski, and Q. Deng. 2018. MicroRNA-223 suppresses the canonical NF-κB pathway in basal keratinocytes to dampen neutrophilic inflammation. Cell Rep 22:1810–1823.